International Journal of Science and Research (IJSR)
ISSN (Online): 2319-7064
Index Copernicus Value (2016): 79.57 | Impact Factor (2017): 7.296

ANN Based HVDC Controller for Frequency Regulation of Power Systems with Wind Generation

Muthyala Lokesh[1], D. J. V. Prasad[2]

[1, 2]SRKR Engineering College, EEE Department, Bhimavaram, India

Abstract: ***This paper deals with the development of a Mat lab-simulink model of a new proposed scheme for grid connected off shore wind farm (OWF) on a VSC-HVDC Converter. The purpose of this simulation Model to getting better damping enhancement and voltage control. An equivalent PMSG is used here to operate the Off shore wind farm A frequency-domain approach based on a linearized system model using PQ theory techniques and a time-domain scheme based on a nonlinear system model subject to various disturbances are both employed to simulate the effectiveness of the proposed control scheme. In this paper we also implement the concept of artificial neural network, applied to the control strategy of HVDC controller. As the artificial neural network has the capability of better controlling of the system compared with the other conventional controllers. It can be concluded from the simulated results that the proposed ANN based HVDC joined with the designed damping controller is very effective to Balance the studied system under disturbance conditions.***

1. Introduction

During the last decades, Wind Energy Conversion System (WECS) has grown dramatically. Variable-speed wind Turbines (VSWTs) attracts considerable interest around the world, which is one of the solutions with the highest potential to reduce wind energy cost. The VSWT systems are usually based on doubly fed induction generators (DFIGs) or permanent magnet synchronous generators (PMSGs). Basically wind farm consists of many wind turbines that are connected with each other to produce small amount of electrical power that becomes powerful after connecting with the transformer. Areas that consists of the number of wind turbines for the sake of power generation from wind and are connected with each other in the different way is called wind farm. Basically wind farm consists of many wind turbines that are connected with each other to produce small amount of electric power. Different strategies are used to build the wind farms in different locations or area. Generators driven by marine-current turbine (MCT) combined with offshore generators driven by wind turbine (WT) will become a novel scheme for energy production in the future. Since oceans cover more than 70% surface of the earth, a hybrid power generation system containing both offshore wind farm (OWF) can be extensively developed at the specific locations of the world in the future. One of the simple methods of running an OWF is to connect the output terminals of several DFIGs together and then connect to a power grid through an offshore step-up transformer and undersea cables. To run an MCF may use several Permanent Magnets synchronous generators (PMSGs) connected directly to the power grid through an offshore step-up transformer and undersea cables. This paper is organized as below. The configuration and the employed models for the studied integrated OWF with HVDC are introduced first [1].

Then, the design procedure and design results for the PID damping controller of the proposed HVDC using pole-placement technique are depicted. Both steady-state operation points under various wind speeds and marine-current speeds and the comparative dynamic responses of the studied system with the designed PID damping controller under different operating conditions can be elaborately done here. This paper proposes the concept of ANN. Generally, Artificial Neural Networks are relatively crude electronic models based on the neural structure of the brain. The brain basically learns from experience. It is natural proof that are beyond the scope of current computers are indeed solvable by small energy efficient packages. This brain modeling also promises a less technical way to develop machine solutions.

2. Modelling of the Proposed System

The offshore wind farm is composed of a group of WT-PMSG as a cluster. This structure manages wind energy and function like a conventional power plant. The load is not directly connected to the wind farm, but it is indirectly connected via the B2B HVDC

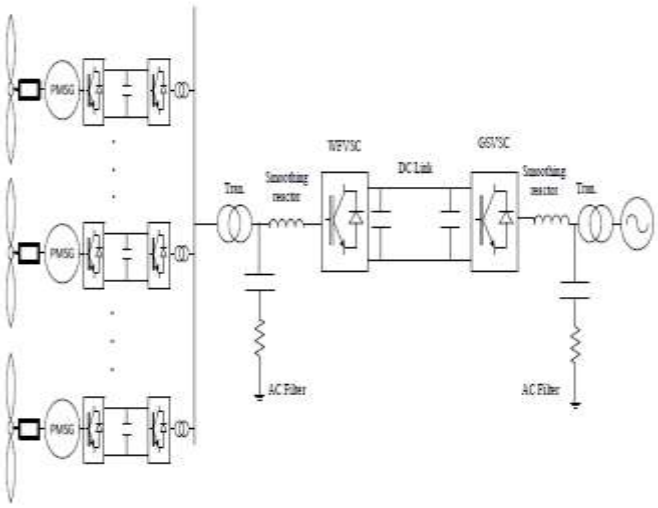

Figure 1: Proposed system with OWF along with HVDC

system. Thus, the wind farm can operate at similar or different frequencies. A VSC-HVDC uses a self-commutated switch such as IGBT with anti-parallel freewheeling diodes to convert the AC/DC power transformation. The DC capacitor on both sides aims to maintain the power balance between AC and DC powers and

reduce the harmonics on the DC side. The coupling transformer and smoothing reactors and AC harmonic filters are connected to the AC bus on both sides and the DC cables.

3. Off Shore Wind Turbine

Wind Energy System

The generation of electrical power is obtained mainly in two ways i.e one is conventional source and other is non-conventional energy sources. The generation of electricity using non-renewable resources such as coal, natural gas, oil and so on, shows great impact on the environment by production of pollution from their general gases. Hence, by considering all these conditions the generation of electricity is obtained from the renewable energy sources. The typical layout of wind power generation as shown below.

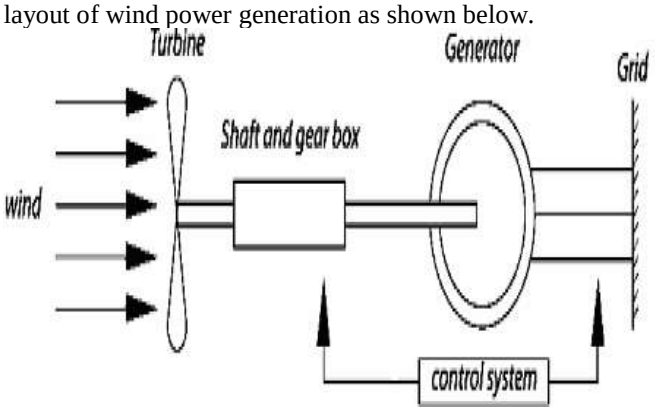

Figure 2: basic schematic diagram of wind turbine

Basically, out of all renewable energy sources the wind turbine plays an important role for generating electricity. Mostly, in present world 50-60 percent of energy is generated from wind turbine as compared with all other renewable energy sources. The mechanical power (in W) produced by a WT can be expressed by

$$P_{mw} = \frac{1}{2}\rho_w A_{rw} V_W^3 C_{pw}(\lambda_w, \beta_w) \qquad (1)$$

Where ρ is the air density in kg/m, Arw is the blade impact area in m2, Vw is the wind speed in m/s, and Cp is the power coefficient of the WT.

Permanent Magnet SG

A synchronous machine is an ac rotating machine whose speed under steady state condition is proportional to the frequency of the current in its armature. Figure 3 indicates the PMSM Cylindrical rotor and Salient rotor structures. The magnetic field created by the armature currents rotates at the same speed as that created by the field current on the rotor, which is rotating at the synchronous speed, and a steady torque results.

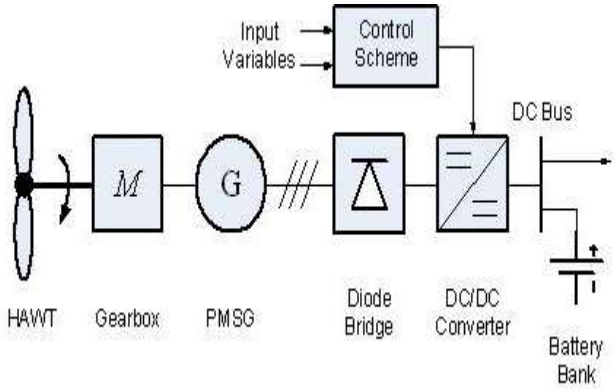

Figure 3: Modelling of PMSG based OWF

Synchronous machines are commonly used as generators especially for large power systems, such as turbine generators and hydroelectric generators in the grid power supply. Because the rotor speed is proportional to the frequency of excitation, synchronous motors can be used in situations where constant speed drive is required. Because the rotor speed is proportional to the frequency of excitation, synchronous motors can be used in situations where constant speed drive is required. Since the reactive power generated by a synchronous machine can be adjusted by controlling the magnitude of the rotor field current, unloaded synchronous machines are also often installed in power systems solely for power factor correction. The armature winding of a conventional synchronous machine is almost invariably on the stator and is usually a three phase winding. Detailed modelling of PM motor drive system is required for proper simulation of the system. The d-q model has been developed on rotor reference frame shown in Figure 4. At any time t, the rotating rotor d-axis makes and angle with the fixed stator phase axis and rotating stator mmf makes an angle ± with the rotor d-axis [13]. Stator mmf rotates at the same speed as that of the rotor.

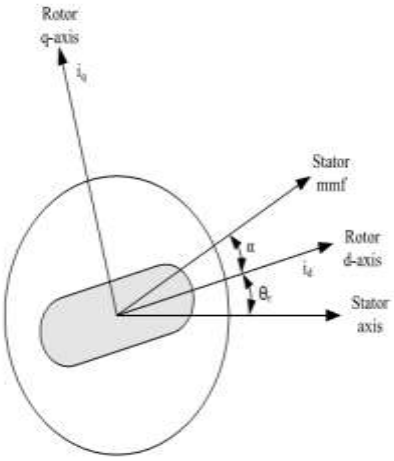

Figure 4: d-q model for the rotor reference frame

The mathematical modelling is obtained by considering the KVL equations for figure 4.

$$V_a = i_a r_a + L\frac{di_a}{dt} + e_a \qquad (2)$$

$$V_b = i_b r_b + L\frac{di_b}{dt} + e_b \qquad (3)$$

$$V_c = i_c r_c + L\frac{di_c}{dt} + e_c \qquad (4)$$

For solving these equations, in this paper we used a concept of line to line parks transformation technique. These parks transformation converts the three phase voltages to two phase coordinators and is expressed as,

$$\begin{bmatrix} V_{ab} \\ V_{ca} \end{bmatrix} = \begin{bmatrix} -\frac{1}{3} & \frac{1}{3} \\ \frac{\sqrt{3}}{3} & -\frac{\sqrt{3}}{3} \end{bmatrix} \begin{bmatrix} V_a \\ V_b \\ V_c \end{bmatrix} \quad (5)$$

The matrix coordinators obtained from the above line to line parks transformation are transformed to orthogonal matrix coordinators (α, β).

Similarly, same like as voltage, the three phase currents also transformed to two phase orthogonal matrix. These two phase currents (I_α, I_β) and voltage (V_α, V_β) are used for calculating the flux linkages (ψ_α, ψ_β) from the expression described as,

And from this equation the phase angle is calculated as,

$$\theta = \tan^{-1}(\Psi_\beta / \Psi_\alpha) \quad (6)$$

$$\Psi_\alpha = \frac{1}{L_\alpha}(V_\alpha - i_\alpha r_\alpha) \quad (7)$$

$$\Psi_\beta = \frac{1}{L_\beta}(V_\beta - i_\beta r_\beta) \quad (8)$$

From the definition of newton's law of motion, the total applied torque is equal to sum of all individual torques across each element.

$$T_e = T_m + J\frac{dw_m}{dt} + Bw_m \quad (9)$$

The electromagnetic torque produced by a brushless dc motor can be expressed as

$$T_e = \frac{e_a i_a + e_b i_b + e_c i_c}{w_m} \quad (10)$$

Assuming the windings of the three phases are symmetrical, the magnitudes of back emfs and currents should be equal for three phases. From the above two equations, the electromagnetic torque can be developed by a BLDC motor at any instant is

$$T_e = \frac{2e_p i_p}{w_m} \quad (11)$$

Where e_p is called phase back emf and i_p is a non-zero phase current.

VSC-HVDC Converter

The grid side converter control stabilizes the dc link voltage at its nominal value. The selection of the DC link voltage (VDC) depends on the value of the L-L rms voltage at the grid side (Vg-LL). The relation is: VDC > 1.633 Vg-LL. In order to realize a transfer of active power generated by the PMSG to the grid, the capacitor voltage is varied during wind turbine operations.

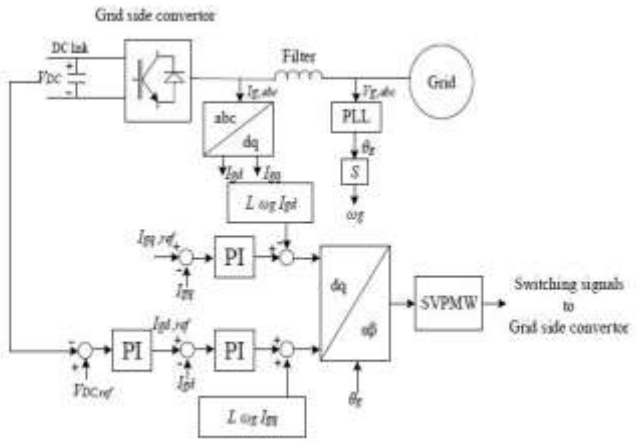

Figure 5: Offshore Wind Farm Voltage Source Converter-HVDC

The control structures developed in this work use PI controllers, since they perform well controlling dc variables. It can be seen in Figure 5 that the outer loops control the dc voltage by taking the dc voltage reference of VDC ref, while the error signal produce Igd reference to inner current control loop that controls active power. The second channel controls the reactive power by producing Igq reference to the inner current control loop. The reactive power is set equal to zero.

Over frequency Controller

Fundamentally, the over frequency controller reduces the current active power generation with a 40% gradient of the presently available power per hertz if the measured frequency exceeds 50.2 Hz .While coordinated with the ancillary frequency control of VSC-HVDC, a participation coefficient Kover has been employed to offset the influence of regulation of VSC-HVDC on the peak frequency during over frequency disturbances

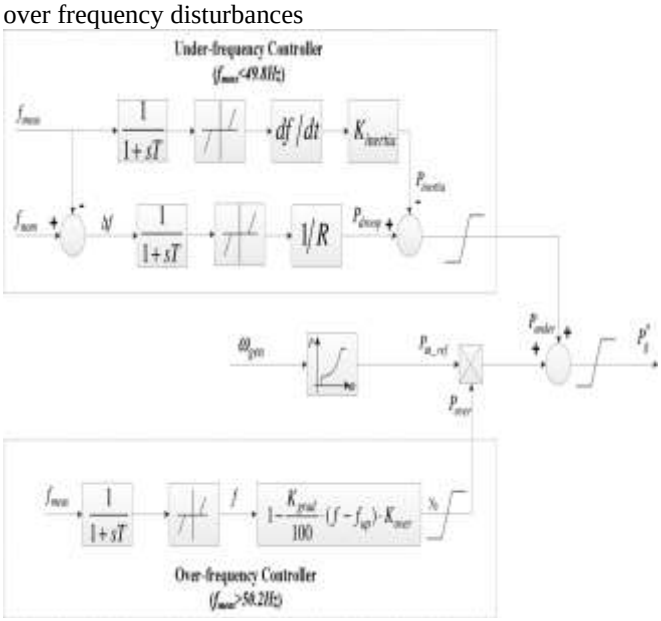

Figure 6: Ancillary frequency controller for FCWT

The control is described as

$$y_o = 1 - K_{grad} * (f - f_{up}) * K_{over} \quad (12)$$

Under frequency Controller

The under frequency controller is used to enable the FCWT to provide inertial response and release active power reserve if applicable, when the system frequency drops lower than 49.8 Hz (nominal 50 Hz) that is determined by the author in the simulation experiments. From Fig 6, it can be seen that the under frequency controller is also composed of two components inertia controller and droop controller.

A demonstrative diagram of the under frequency controller is shown in Fig 7. The inertia controller is applied to emulate the inertial response of SGs and its output active power reference Pinertia is proportional to the derivative of the system frequency. The droop controller is applied to emulate the response of the speed governor of a SG, and its output active power reference Pdroop is proportional to the absolute deviation of the system nominal frequency.

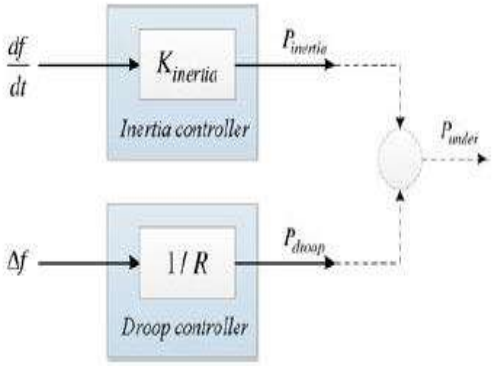

Figure 7: Under frequency controller

4. Artificial Neural Networks

Figure 8 shows the structure of an ANN, in which fixed node indicated by a circle, an adaptive node indicated by square. In this structure hidden layers are presented in between input and output layer, these nodes are functioning as membership functions and the rules obtained based on the if-then statements is eliminated [7]. For simplicity, we considering the examined ANN has two inputs and one output. In this network, each neuron and each element of the input vector p are connected with weight matrix W. The hybrid learning algorithms are implemented for obtaining the values of system parameters. These learning algorithms is a function of linear and non-linear parameters. These explanations are implemented in Matlab/Simulink software.

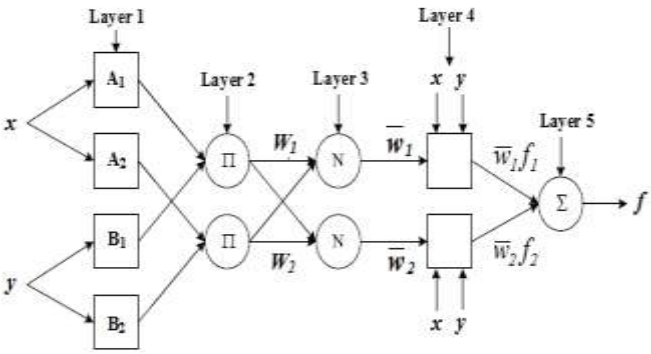

Figure 8: ANN architecture for a two-input multi-layer network

Where the two crisp inputs are x and y, the linguistic variables associated with the node function are Ai and Bi. The system has a total of five layers are shown in Fig 8.

5. Simulation Diagram & Results

The proposed system is simulated as from the circuit shown in figure 1 by applying ANN Controller. A large FCWT-based OWF rated at 135 MW is integrated into the grid via VSC-HVdc on Bus 5 (PCC).The VSC converter has two back to back converters as shown in figure. One converter connected offshore windfarm termed as offshore converter and other termed as onshore converter.

Results for proposed system with ANN over frequency event

The simulation results for the sudden load decrease scenario are shown in Fig 9. These results obtained for the designed power system for three different cases shown in the simulation.

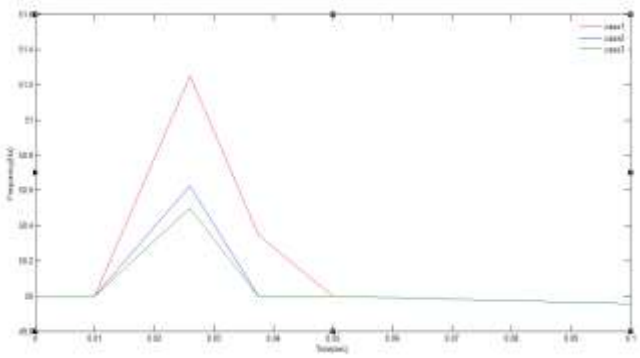

Figure 9 (a): System frequency Response

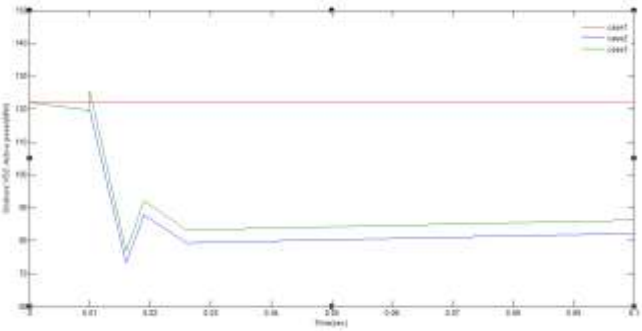

Figure 9 (b): OWT Active power

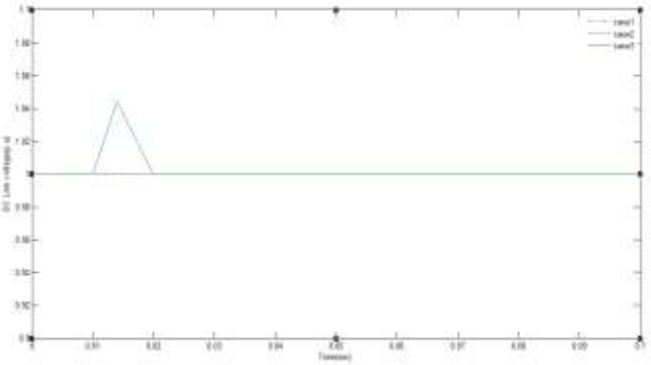

Figure 9 (c): HVDC DC- link Voltage

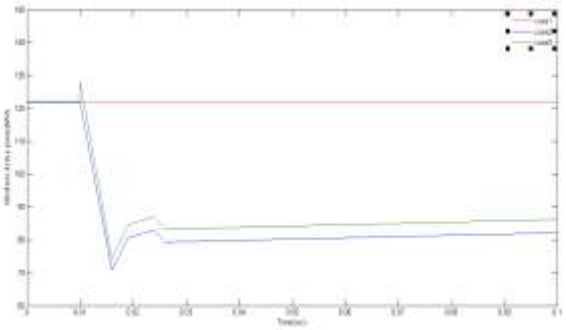

Figure 9 (d): Onshore VSC active power

The system frequency response is shown in Fig. 9 (a). It can be seen that the frequency support provided only by the offshore wind farm does not improve the initial frequency dynamics but reduces the peak frequency and achieves significant enhancement on the frequency restoration. The joint frequency support provided by both offshore wind farm and VSC-HVDC further lowers down the peak frequency more obviously.

Fig. 9 (b) presents the offshore wind farm generation regarding the given over frequency event. According to (3), the reduction in the offshore wind farm generation is proportional to the over frequency deviation. As above mentioned, the VSC HVDC support reduces the peak frequency. However, it, in turn, covers the actual severity of the frequency variation to FCWTs and, thus, weakens the FCWTs' frequency support as the Pink curves illustrate in Fig. 9 (a) and (b). Fig. 9 (c) and (d) presents the response of VSC-HVDC for the sudden load reduction. It can be observed from Fig.9 that in the frequency-rising period, the dc voltage is controlled to increase to let the dc capacitors charge and absorb energy that slows down the ROCOF and reduces the absolute frequency deviation. After the offshore wind farm reduces its generation as a response to the over frequency as shown in Fig. 9 (b), the dc voltage begins to drop [see Fig. 9 (c)], and the dc capacitors then begin to discharge and release energy that impairs the frequency restoring. The charging and discharging of dc capacitance are reflected in the active power output of onshore VSC as shown in Fig. 9 (d).

6. Results for proposed system with ANN under frequency event

The simulation results for the sudden load increase scenario are shown in Fig.10. These results obtained for the designed power system for three different cases shown in the simulations.

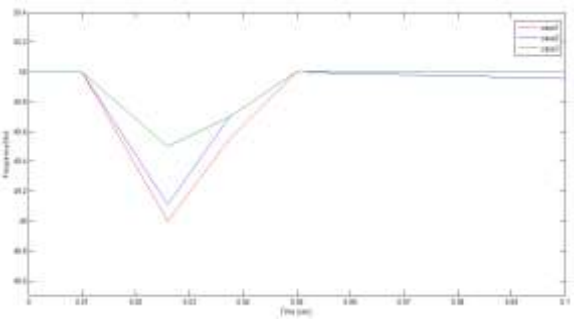

Figure 10 (a): System frequency Response

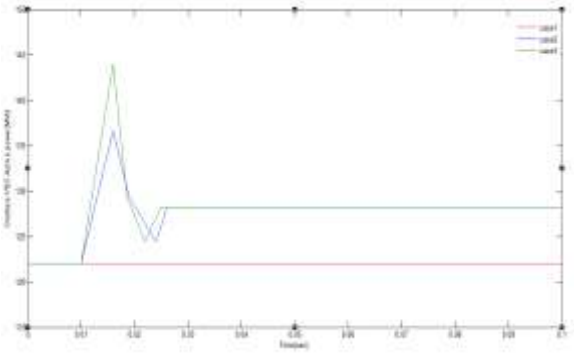

Figure 10 (b): OWT Active power

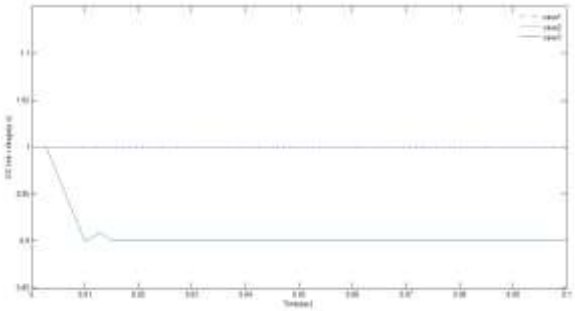

Figure 10 (c): HVDC DC- link Voltage

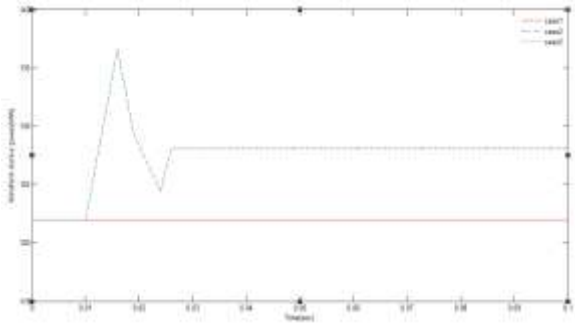

Figure 10 (d): Onshore VSC active power

The frequency response of the ac power system is shown in Fig 10(a). It is observed that the frequency support from the offshore wind farm makes up active power for the load increase and reduces the frequency drop significantly.

The offshore wind farm generation is shown in Fig 10(b). It can be seen that if the ancillary frequency controller is not activated, the operation of FCWTs is not affected due to the decoupling of converters. In the cases that the frequency controller of FCWTs is activated, it can be observed that at the instant that the frequency drop is detected by the FCWTs, there is a sudden increase of the active power generation of the offshore windfarm. The participation of VSC-HVDC in the frequency regulation does not exert evident influence on the generation of the OWF.

Fig 10(c) presents the response of VSC-HVDC for the load increase .When the ancillary frequency controller of VSC-HVDC is activated, the dc voltage is controlled to drop down to 0.9 p.u. quickly as shown in Fig. 9 (c) to release part of the power stored in dc capacitance.

Fig 10(d) presents the response of VSC-HVDC for the load increase. It can be seen from curves of Case 2 that the onshore VSC increases its active power output as offshore wind farm starts to generate more power to support the

frequency, while only offshore wind farm responds to the frequency decline. In consequence, the onshore VSC is able to infeed more active power into the onshore grid to support the frequency as illustrated in Fig 10(d). This coordinated frequency regulation of offshore wind farm and VSC-HVDC obtains better frequency response as mentioned above

7. Conclusion

The main focus of this paper has been the study and control of a direct-driven PMSG used in variable speed wind energy system connected to the grid. This wind system was modelled using d-q rotor reference frame and is interfaced with the power system through an inverter and a filter modelled in the power system reference frame. This paper has presented the dynamic stability improvement of an integrated OWF using a HVDC. A PID damping controller has been designed for the HVDC by using a unified approach based on pole-assignment approach. Eigen value calculations and time domain simulations of the studied system subject to a noise wind-speed disturbance, a marine current speed disturbance, and a three-phase short circuit fault at the grid have been systematically performed to demonstrate the effectiveness of the proposed HVDC joined with the ANN damping controller on suppressing voltage fluctuation of the studied system and improving system dynamic stability under different operating conditions. It can be concluded from the simulation results that the proposed HVDC joined with the ANN damping controller is capable of improving the performance of the studied integrated OWF under different operating conditions.

References

[1] S. E. B. Elghali, R. Balme, K. L. Saux, M. E. H. Benbouzid, J. F. Charpentier, and F. Hauville, "A simulation model for the evaluation of the electrical power potential harnessed by a marine current turbine," IEEE J. Ocean. Eng., vol. 32, no. 4, pp. 786–797, Oct. 2007.
[2] W. M. J. Batten, A. S. Bahaj, A. F. Molland, and J. R. Chaplin, "Hydro-dynamics of marine current turbines," Renewable Energy, vol. 31, no. 2, pp. 249–256, Feb. 2006.
[3] L. Myers and A. S. Bahaj, "Simulated electrical power potential harnessed by marine current turbine arrays in the Alderney race," Renewable Energy, vol. 30, no. 11, pp. 1713–1731, Sep. 2005.
[4] H. Chong, A. Q. Huang, M. E. Baran, S. Bhattacharya, W. Litzenberger, L. Anderson, A. L. Johnson, and A. A. Edris, "STATCOM impact study on the integration of a large wind farm into a weak loop power system," IEEE Trans. Energy Convers., vol. 23, no. 1, pp. 226–233, Mar. 2008.
[5] H. Gaztanaga, I. Etxeberria-Otadui, D. Ocnasu, and S. Bacha, "Real-time analysis of the transient response improvement of fixed-speed wind farms by using a reduced-scale STATCOM prototype," IEEE Trans. Power Syst., vol. 22, no. 2, pp. 658–666, May 2007.
[6] T. Y. Lee, "Operating schedule of battery energy storage system in a time-of-use rate industrial user with wind turbine generators: A multipass iteration particle swarm optimization," IEEE Trans. Energy Convers., vol. 22, no. 3, pp. 774–782, Sep. 2007.
[7] R. S. Bhatia, S. P. Jain, D. K. Jain, and B. Singh, "Battery energy storage system for power conditioning of renewable energy sources," in Proc. Int. Conf. Power Electron. Drive Syst., Jan. 2006, vol. 1, pp. 501–506.
[8] D. J. Swider, "Compressed air energy storage in an electricity system with significant wind power generation," IEEE Trans. Energy Convers., vol. 22, no. 1, pp. 95–102, Mar. 2007.
[9] S. Nomura, Y. Ohata, T. Hagita, H. Tsutsui, S. Tsuji-Iio, and R. Shimada, "Wind farms linked by SMES systems," IEEE Trans. Appl. Supercond., vol. 15, no. 2, pp. 1951–1954, Jun. 2005.
[10] K. Shikimachi, H. Moriguchi, N. Hirano, S. Nagaya, T. Ito, J. Inagaki, S. Hanai, M. Takahashi, and T. Kurusu, "Development of MVA class HTS SMES system for bridging instantaneous voltage dips," IEEE Trans. Appl. Supercond., vol. 15, no. 2, pp. 1931–1934, Jun. 2005.